

Two-phonon wobbling in  $^{135}\text{Pr}$ 

N. Sensharma<sup>a</sup>, U. Garg<sup>a,\*</sup>, S. Zhu<sup>b</sup>, A.D. Ayangeakaa<sup>b,1</sup>, S. Frauendorf<sup>a</sup>, W. Li<sup>a,c</sup>, G.H. Bhat<sup>d</sup>, J.A. Sheikh<sup>e</sup>, M.P. Carpenter<sup>b</sup>, Q.B. Chen<sup>f</sup>, J.L. Cozzi<sup>a</sup>, S.S. Ghugre<sup>g</sup>, Y.K. Gupta<sup>a,h</sup>, D.J. Hartley<sup>i</sup>, K.B. Howard<sup>a</sup>, R.V.F. Janssens<sup>j,k</sup>, F.G. Kondev<sup>b</sup>, T.C. McMaken<sup>a,2</sup>, R. Palit<sup>l</sup>, J. Sethi<sup>b</sup>, D. Seweryniak<sup>b</sup>, R.P. Singh<sup>m</sup>

<sup>a</sup> Physics Department, University of Notre Dame, Notre Dame, IN 46556, USA

<sup>b</sup> Physics Division, Argonne National Laboratory, Argonne, IL 60439, USA

<sup>c</sup> NSCL, Michigan State University, East Lansing, MI 48824, USA

<sup>d</sup> Department of Physics, Government Degree College, Kulgam 192 231, India

<sup>e</sup> Cluster University, Srinagar, Jammu and Kashmir, 190 008, India

<sup>f</sup> Physik-Department, Technische Universität München, D-85747 Garching, Germany

<sup>g</sup> UGC-DAE Consortium for Scientific Research, Kolkata 700 064, India

<sup>h</sup> Nuclear Physics Division, Bhabha Atomic Research Center, Mumbai 400 085, India

<sup>i</sup> Department of Physics, United States Naval Academy, Annapolis, MD 21402, USA

<sup>j</sup> Department of Physics and Astronomy, University of North Carolina at Chapel Hill, Chapel Hill, NC 27599, USA

<sup>k</sup> Triangle Universities Nuclear Laboratory, Duke University, Durham, NC 27708, USA

<sup>l</sup> Department of Nuclear and Atomic Physics, Tata Institute of Fundamental Research, Mumbai 400 005, India

<sup>m</sup> Inter University Accelerator Centre, Aruna Asaf Ali Marg, New Delhi 110 067, India

## ARTICLE INFO

## Article history:

Received 18 December 2018

Received in revised form 2 February 2019

Accepted 20 March 2019

Available online 22 March 2019

Editor: D.F. Geesaman

## ABSTRACT

The second-phonon ( $n_\omega = 2$ ) wobbling band has been established in the nucleus  $^{135}\text{Pr}$ . Conclusive evidence for its wobbling nature comes from the  $\Delta I = 1$ , E2 character of the transitions between the new band and the previously identified transverse wobbler band ( $n_\omega = 1$ ) in this nucleus. Theoretical calculations in the framework of the quasiparticle triaxial rotor and triaxial projected shell models are found to be in good agreement with the experimental results.

© 2019 The Author(s). Published by Elsevier B.V. This is an open access article under the CC BY license (<http://creativecommons.org/licenses/by/4.0/>). Funded by SCOAP<sup>3</sup>.

Triaxiality is a rather rare and interesting phenomenon in nuclear physics. While many experimental characteristics are said to be resulting from such a shape [1], the only unambiguous experimental consequences of triaxiality are chirality [2] and wobbling [3]. While chirality is already a well-established phenomenon in that a large number of chiral bands have now been observed over many parts of the nuclear periodic table [4], the experimental observation of nuclear wobbling motion has been rare so far. Indeed, wobbling bands have been reported in only 8 nuclei—5 in the  $A \sim 160$  region [5–9], 2 in the  $A \sim 130$  region [10,11], and, very recently, 1 in the  $A \sim 100$  region [12].

\* Corresponding author.

E-mail address: [garg@nd.edu](mailto:garg@nd.edu) (U. Garg).

<sup>1</sup> Present Address: Department of Physics, United States Naval Academy, Annapolis, MD 21402, USA.

<sup>2</sup> Research Experience for Undergraduates (REU) Program student from Case Western Reserve University, Cleveland, OH 44106, USA.

The notion of wobbling motion of an even-even triaxial nucleus was introduced by Bohr and Mottelson [3], describing it as the oscillation of one of the principal axes of a triaxial rotor about the space-fixed angular momentum vector. The mode is the quantum mechanical analog of the oscillation of one of the principal axes of a classical asymmetric top. Bohr and Mottelson considered the ideal case of harmonic oscillations, which appears as the small-amplitude limit of the exact eigenfunctions of the triaxial rotor Hamiltonian [3]. In accordance with the interpretation of nuclear vibrations, wobbling excitations are also classified by their phonon number when their structure deviates from the harmonic limit [13,14]. Wobbling bands are experimentally observed as multiple rotational bands, each corresponding to a particular wobbling phonon number  $n_\omega$  where  $n_\omega = 0, 1, 2, \dots$  etc. The spin sequence is  $I = \alpha + 2n$  for an even number of wobbling quanta and  $I = \alpha + 2n + 1$  for an odd number. The signature  $\alpha$  of the zero-phonon band is 0 for even-even nuclei and  $\pm 1/2$  for odd-A nuclei, depending on the structure of the odd quasiparticle. These

$n_\omega$ -bands are connected via  $\Delta I = 1$  transitions, which, due to the collective nature of wobbling excitations, exhibit a dominant E2 character.

Hamamoto and coworkers were the first to study wobbling in odd-A nuclei [5,13]. In this case, the states  $n_\omega = 0, 2, \dots$  and  $n_\omega = 1, 3, \dots$  have the respective spin sequence  $I = \alpha + \text{even number or odd number}$ , where  $\alpha = \pm 1/2$  is the favored (unfavored) signature of the odd quasiparticle. For the present case of the  $h_{11/2}$  quasi proton in  $^{135}\text{Pr}$ , it is  $\alpha = -1/2$ .

The wobbling frequency characterizes the type of wobbling excitation. For an even-even nucleus, this frequency increases with increasing spin. However, for an odd-mass nucleus, Frauendorf and Dönau showed that two possibilities exist [14]: a longitudinal wobbler (the odd-particle aligned parallel to the axis of maximum moment of inertia, the “medium axis”) and a transverse wobbler (the odd-particle aligned perpendicular to the axis of maximum moment of inertia, the “short axis”). Using the Quasiparticle Triaxial Rotor (QTR) model, they showed that longitudinal wobbling is characterized by an increasing wobbling energy ( $E_{\text{wobb}}$ ) with increasing angular momentum, whereas for transverse wobbler,  $E_{\text{wobb}}$  decreases instead [14]. They applied the classification of one-, two-, ... wobbling phonon excitations to the QTR solutions, as long as they have the same topology as the harmonic limit from which they quantitatively deviate.

In addition to the one-phonon wobbling band there exists a second band with signature opposite to that of the yrast band. This “unfavored signature partner” represents the energetically less favored coupling of the odd particle with the uniformly rotating rotor. The signature partner (SP) band exist both in axial and triaxial nuclei. In the latter case, the wobbling band appears in addition; this band is distinguished from the SP band by its large quadrupole transitions to the yrast band.

For a long time, only five cases of wobbling motion were experimentally established, all in the  $A \sim 160$  region:  $^{161}\text{Lu}$  [8],  $^{163}\text{Lu}$  [5],  $^{165}\text{Lu}$  [6],  $^{167}\text{Lu}$  [7] and  $^{167}\text{Ta}$  [9]. Just about three years ago, a wobbling band was observed in the nucleus  $^{135}\text{Pr}$  [10], establishing a new region of the nuclear chart where this phenomenon was shown to exist. It has since been followed by another case in this new region,  $^{133}\text{La}$  [11] and, more recently, in  $^{105}\text{Pd}$  [12]. The alignment necessary to undergo wobbling in nuclei in the  $A \sim 130$  mass region is provided by an  $h_{11/2}$  proton coupled to a core with a relatively small deformation of  $\epsilon \sim 0.16$  [10,11], in contrast with the wobblers in the  $A \sim 160$  region, where the aligned particle is an  $i_{13/2}$  proton and the core has a larger deformation of  $\epsilon \sim 0.40$  [10].

With the possible exception of  $^{133}\text{La}$ ,  $E_{\text{wobb}}$  for all the wobblers discovered so far has been found to follow a decreasing trend with increasing spin, establishing these as transverse wobblers.  $^{133}\text{La}$ , on the other hand, appears to exhibit properties of a longitudinal wobbler [11].

As stated previously, several wobbling bands (corresponding to different  $n_\omega$  values) may occur in a nucleus and, indeed, observation of wobbling bands corresponding to higher  $n_\omega$  values provides a further and clear validation of the wobbling scenario. However, there have been only two cases so far where wobbling bands corresponding to higher phonons ( $n_\omega = 2$ ) have been identified:  $^{163,165}\text{Lu}$  [15,6]. In this Letter, we report identification of the second-phonon ( $n_\omega = 2$ ) wobbler band (hereafter termed the TW2 band) in  $^{135}\text{Pr}$ . The wobbling character of the band is established by ascertaining the  $\Delta I = 1$ , E2 character of the transitions between this band and the previously-reported  $n_\omega = 1$  band (hereafter termed the TW1 band). Furthermore, the experimentally observed properties of these bands are in consonance with theoretical expectations.

**Table 1**

DCO-like ratios ( $r$ ) for the transitions corresponding to the TW2  $\rightarrow$  TW1, and the SP  $\rightarrow$  Yrast transitions.

$n_\omega = 2$		Signature partner	
Energy (keV)	$r$	Energy (keV)	$r$
450.2	$0.55 \pm 0.03$	702.3	$0.86 \pm 0.04$
550.5	$0.49 \pm 0.10$	767.7	$0.90 \pm 0.08$
517.1	$0.37 \pm 0.20$	758.4	$0.92 \pm 0.22$

Details of the measurement are very similar to those reported in Ref. [10] and are only briefly recapitulated here. An 80-MeV beam of  $^{16}\text{O}$  was produced using the ATLAS facility at the Argonne National Laboratory. It was incident on a  $^{123}\text{Sb}$  target to populate the levels of interest in  $^{135}\text{Pr}$ . The target used was a  $634 \mu\text{g}/\text{cm}^2$ -thick foil of  $^{123}\text{Sb}$  with a  $15 \mu\text{g}/\text{cm}^2$  aluminum layer at the front. At the time of the experiment, the Gammasphere array had 83 working Compton-suppressed Germanium detectors arranged in 17 different angular rings around the beam line. Data was acquired in the triple coincidence mode. The upgrade to the digital Gammasphere (DGS) enabled collection of nearly 4 times as much data as that in Ref. [10] in a similar amount of beam time—a total of  $1.45 \times 10^{10}$  three and higher-fold  $\gamma$ -ray coincidence events. The data was analyzed using the RADWARE suite of codes [16]. Energy and efficiency calibrations were performed for each of the working detectors of the Gammasphere array using a standard  $^{152}\text{Eu}$  radioactive source.

The calibrated data was then sorted into  $\gamma$ - $\gamma$  coincidence matrices and  $\gamma$ - $\gamma$ - $\gamma$  coincidence cubes. The high statistics afforded by DGS enabled the construction of an elaborate level scheme of  $^{135}\text{Pr}$ ; only the parts relevant to this report are shown in Fig. 1. In addition to the previously reported Yrast sequence, the TW1 band, its signature partner (SP), and the dipole band, the present work has identified the TW2 band with properties very similar to that of TW1. Four connecting transitions between the two wobbling bands have been established. The Yrast and the SP sequences have been extended to higher spins. Spin and parity assignments to the newly added levels have been made on the basis of angular distributions and DCO-like ratios. A complete description of DCO-like ratios can be found in Ref. [17].

Angular distribution measurements for the  $\Delta I = 1$  transitions between the TW2 and TW1 bands were analyzed and the mixing ratios  $\delta$  extracted using standard angular distribution analysis procedures (see, for example, Refs. [10,17,18]). Due to the symmetric arrangement of Gammasphere detectors, the data was sorted into seven rings covering the angular range from  $\theta = 0^\circ$  to  $90^\circ$  with each ring corrected individually for efficiency. The angular distribution curves were then fitted with the standard function given in, for example, Ref. [19]. The fits for the three lowest TW2  $\rightarrow$  TW1 transitions are presented in Fig. 2. These distributions revealed about 78–92% E2 admixtures in the  $\Delta I = 1$  linking transitions, as expected for wobbling bands;  $\delta$ , and the percentage of E2 admixture are included in Fig. 2 as well. It should be noted that this angular distribution analysis procedure was benchmarked for this nucleus in Ref. [10] with transitions of previously-known pure E2 and M1 character. Further details about the procedures will be provided in a forthcoming publication [20].

Further, DCO-like ratios were obtained for the TW2  $\rightarrow$  TW1 linking transitions and the values were found to be very similar to those for the TW1  $\rightarrow$  Yrast connecting transitions in Ref. [17]. The DCO-like ratios calculated for all the SP  $\rightarrow$  Yrast linking transitions are close to 0.8, the value for a pure dipole transition in the Gammasphere geometry [21]; some of these transitions are too weak to perform full angular distribution analyses. The extracted DCO-like ratios are presented in Table 1.

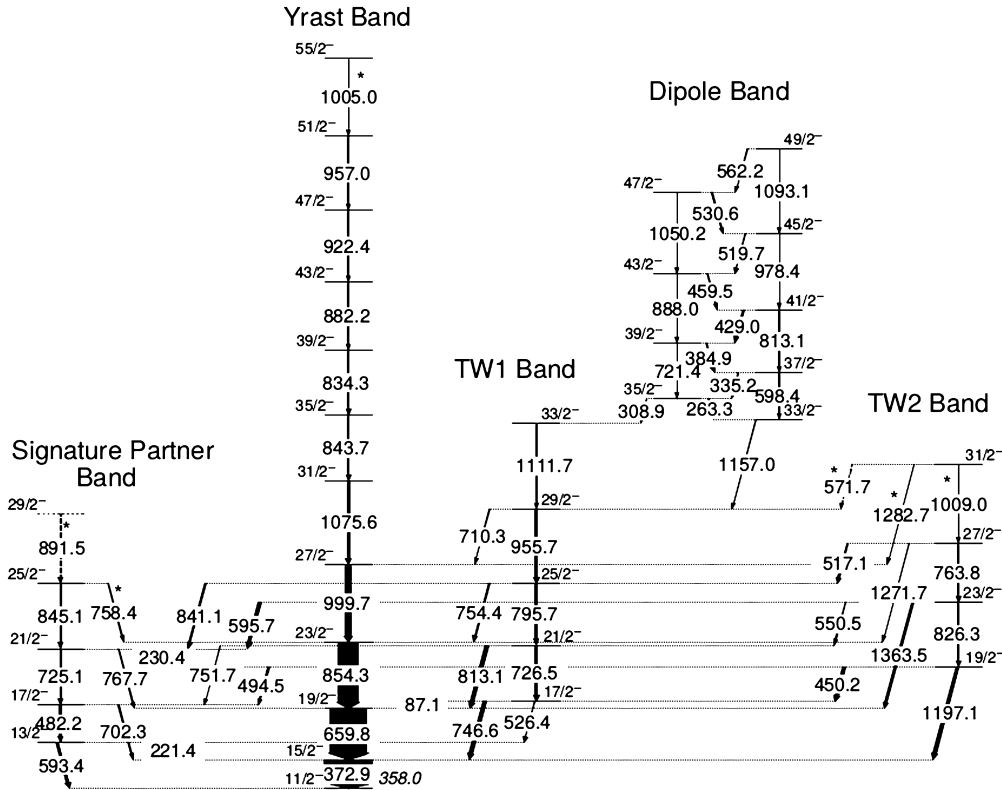


Fig. 1. Partial negative-parity level scheme of  $^{135}\text{Pr}$  developed in the present work. Shown are the previously known Yrast band, the  $n_{\omega} = 1$  wobbling (TW1) band, the signature partner band and a dipole band. Higher statistics allowed identification of a new  $n_{\omega} = 2$  wobbling (TW2) band and the extension of the Yrast band. Newly identified transitions are shown with an asterisk (\*). Tentative  $\gamma$ -ray transitions are shown as dotted lines.

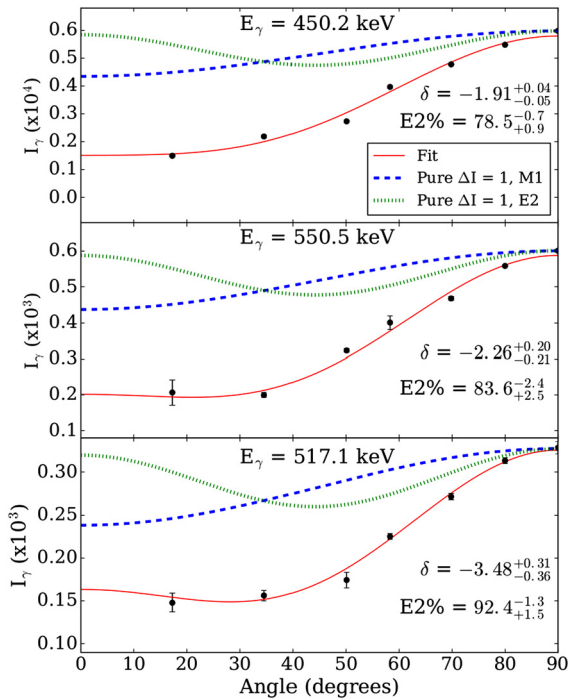


Fig. 2. Angular distribution plots for the three lowest  $n_{\omega} = 2 \rightarrow n_{\omega} = 1$  linking transitions. The mixing ratios and the percentage of E2 admixture are noted on each plot. The results establish a  $\Delta I = 1$ , primarily E2 character for the transitions between wobbling bands.

Another aspect of wobbling bands is high reduced E2 transition probabilities,  $B(E2)_{\text{out}}$  for the  $\Delta I = 1$  linking transitions in compar-

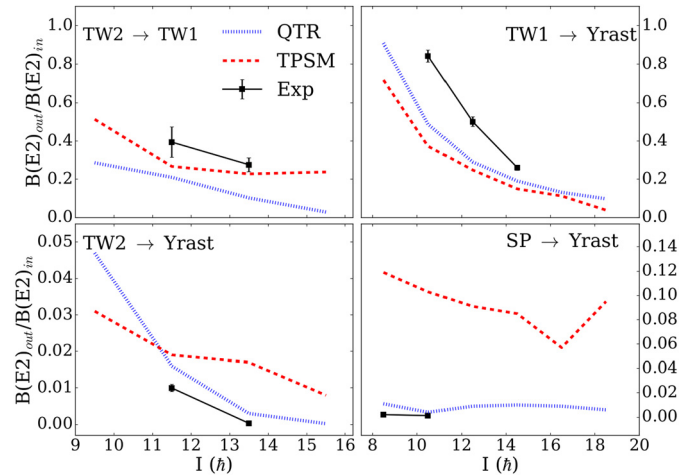
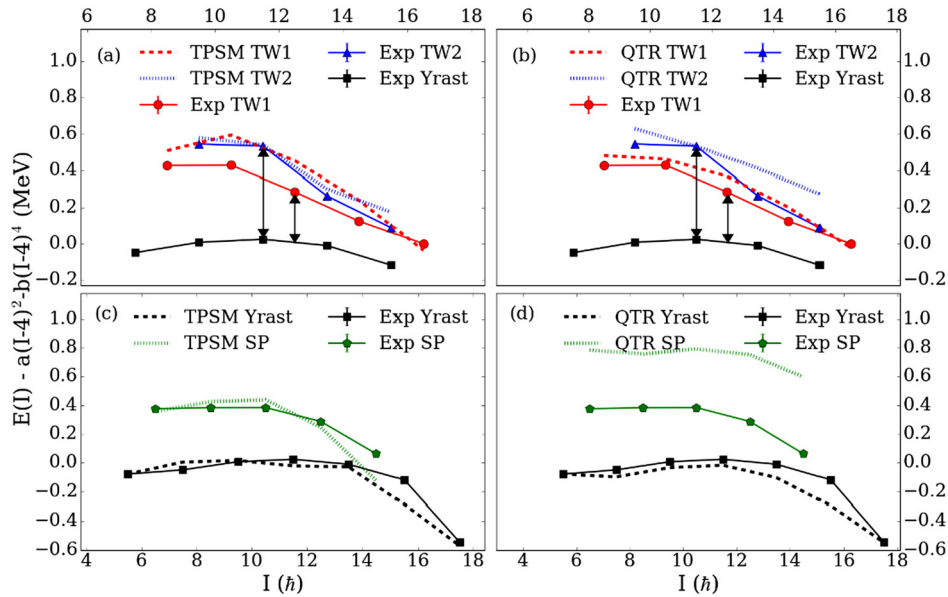


Fig. 3.  $B(E2)_{\text{out}}/B(E2)_{\text{in}}$  vs. spin for the TW2  $\rightarrow$  TW1, TW1  $\rightarrow$  Yrast, TW2  $\rightarrow$  Yrast and the SP  $\rightarrow$  Yrast transitions. (TPMSM (red dashed line), QTR (blue dotted line) and experiment (black squares connected by black solid line). Experimental values for TW1  $\rightarrow$  Yrast taken from Ref. [10].

ison with those for the in-band  $\Delta I = 2$  transitions,  $B(E2)_{\text{in}}$ . While it was not possible to measure absolute transition probabilities in this work, the  $B(E2)_{\text{out}}/B(E2)_{\text{in}}$  ratios could be extracted from the intensities of these transitions, combined with the mixing ratios obtained from angular distributions. These are presented in Fig. 3.

The nature (transverse or longitudinal) of the observed wobbling band can be determined from the behavior of the wobbling energy,  $E_{\text{wobb}}$  as a function of the angular momentum. The wobbling energy  $E_{\text{wobb}}$  is defined as the excitation energy with respect to the Yrast sequence, which is the  $n_{\omega} = 0$  band. These are illus-



**Fig. 4.** Experimental level energies minus a rotor contribution vs. spin, for the TW1, TW2, Yrast and SP bands in  $^{135}\text{Pr}$ . To correct for the aligned particle, an alignment of 4.5 has been subtracted from the rotor contribution i.e.,  $I(I+1) - 4.5 \approx (I + \frac{1}{2} - 4.5)^2 = (I-4)^2$ . The constants  $a = 0.0348$  MeV and  $b = 0.00003$  MeV are empirical. Also shown for comparison are the corresponding numbers as given by TPSM and QTR calculations. Solid lines through the experimental points are drawn to guide the eye. The double pointed arrows between the experimental TW2, TW1 and Yrast points indicate the wobbling energy for the TW2 and the TW1 bands, respectively.

trated by double-pointed arrows in Fig. 4. In the case of the TW1 band, it is taken as the distance to the interpolated value of the adjacent Yrast energies. The decrease of  $E_{\text{wobb}}$  (TW2) as a function of increasing spin clearly identifies this as a case of transverse wobbling, similar to that of  $E_{\text{wobb}}$  (TW1) observed in Ref. [10].

To elucidate and understand the observed TW + SP band structure, calculations were performed employing the Quasiparticle Triaxial Rotor (QTR) model [14], and the Triaxial Projected Shell Model (TPSM) [22]. The interpretation of the QTR results in terms of transverse and longitudinal wobbling modes has been discussed in Ref. [14]. As the TSPM comprises the same physics as the QTR viz. the coupling of the odd quasiparticle with the triaxial rotor core, it is well suited to describe the wobbling modes. Superior to the QTR, the moments of inertia in TSPM are calculated in a microscopic way and the antisymmetrization between the odd valence quasiproton and the quasiparticles forming the rotor is fully taken into account. An analysis of the angular momentum geometry is yet to be carried out.

The QTR calculations are identical to those in Ref. [10], which included pairing and employed the deformation parameters  $\epsilon = 0.16$  and  $\gamma = 26^\circ$  and the moments of inertia  $\mathcal{J}_m$ ,  $\mathcal{J}_s$  and  $\mathcal{J}_l = 7.4$ , 5.6 and  $1.8 \hbar^2/\text{MeV}$ , where, respectively,  $m$ ,  $s$  and  $l$  stands for medium, short and long. Likewise, the moments of inertia had a spin-dependent increase given by the scale factor  $1 + 0.116I$ . The TPSM calculations used deformation parameters  $\epsilon = 0.17$  and  $\epsilon' = 0.12$  (corresponding to  $\gamma = 35^\circ$ ). The moments of inertia are obtained at a microscopic level in this approach.

Fig. 4 provides the energies relative to the Yrast sequence (Y). The TW1 wobbling energy obtained by QTR is somewhat larger than the experiment. As discussed in Ref. [10], it first decreases with the angular momentum,  $I$ , which is the hallmark of transverse wobbling. The increase at the highest value of  $I$  is caused by a transition to longitudinal wobbling. The experimental energies of the TW2 band are substantially lower than twice the energies of the TW1 sequence, which is also the case for the QTR values. This depression of the two-phonon energy signals strong anharmonicity. Fig. 3 displays the ratios  $B(E2)_{\text{out}}$  between two bands and  $B(E2)_{\text{in}}$  within the band of origin. The QTR somewhat underestimates the ratio  $B(E2, \text{TW1}, I \rightarrow Y, I-1)/B(E2, \text{TW1}, I \rightarrow \text{TW1}, I-2)$ ,

while the collective enhancement of the transition is clearly visible. The ratio  $B(E2, \text{TW2}, I \rightarrow \text{TW1}, I-1)/B(E2, \text{TW2}, I \rightarrow \text{TW2}, I-2)$  is smaller than the ratio  $B(E2, \text{TW1}, I \rightarrow Y, I-1)/B(E2, \text{TW1}, I \rightarrow \text{TW1}, I-2)$ , which is in stark contrast to the factor of two expected for a harmonic wobbling mode. The QTR calculations reproduce the small ratio, which is in accordance with the strong anharmonicity seen in the energies. Another consequence of anharmonicity is the existence of  $\text{TW2}, I \rightarrow Y, I-2$  transitions, which is forbidden in the harmonic limit. The rather small  $B(E2, \text{TW2}, I \rightarrow Y, I-2)/B(E2, \text{TW2}, I \rightarrow \text{TW2}, I-2)$  ratio is well reproduced by the QTR. A semiclassical analysis of transverse wobbling suggests strong anharmonicity for the two-phonon state because it comes close to the separatrix, which is the line that separates the transverse regime from the longitudinal one (see Fig. 10 in Ref. [14]).

The results of the TPSM calculations are consistent with the QTR interpretation. The one-phonon wobbling energy is overestimated by a larger amount than by the QTR. This is not surprising because TPSM determines the moments of inertia on a microscopic basis, which are adjustable in the QTR approach. The TPSM suggests an even more anharmonic scenario than QTR and the experiment. The one- and two-phonon wobbling energies are about the same. The ratios of the E2 transition are close to the QTR values indicating anharmonicity of similar strength. The position of the SP band is better reproduced than in case of the QTR.

An important aspect of the wobbling interpretation is the existence of an additional SP band, which represents a dealignment of the  $h_{11/2}$  quasiproton with respect to the  $s$ -axis. It appears as the “unfavored signature partner” in both axial and triaxial nuclei. Only triaxial nuclei develop collective wobbling states, however. Accordingly, no collective E2 enhancement of the transition to the Yrast band is expected for the SP band. As illustrated in Fig. 4, the QTR overestimates the SP energies whereas the TPSM gives about the right values. The low values for the experimental ratio  $B(E2, \text{SP}, I \rightarrow Y, I-1)/B(E2, \text{SP}, I \rightarrow \text{SP}, I-2)$  are reproduced by the QTR calculations. The TPSM gives a larger ratio, which indicates some coupling between the one-phonon wobbling and the SP states. Further details of this problem will be provided in a separate theoretical publication [23].

In summary, we have identified a wobbling band built on  $n_{\omega} = 2$  phonon excitation in the nucleus  $^{135}\text{Pr}$ . This band is connected to the  $n_{\omega} = 1$  wobbling band via four  $\Delta I = 1$  transitions, the high E2 content of which was established from angular distribution measurements. The experimentally observed properties of this band are found to be in good agreement with the calculations in the framework of the TPSM and QTR models. This is the first observation of two-phonon wobbling in the  $A \sim 130$  region, and further strengthens the existence of this phenomenon in a mass region and spin values different from all previously reported cases of wobbling.

### Acknowledgements

This work has been supported by the U.S. National Science Foundation [Grants No. PHY-1713857 (UND), No. PHY-1559848 (UND), and No. PHY-1203100 (USNA)], and by the U. S. Department of Energy, Office of Science, Office of Nuclear Physics [Contract No. DE-AC02-06CH11357 (ANL), No. DE-FG02-95ER40934 (UND), No. DE-FG02-97ER41033 (UNC) and DE-FG02-97ER41041 (TUNL)]. The work of QBC was supported by Deutsche Forschungsgemeinschaft (DFG) and National Natural Science Foundation of China (NSFC) through funds provided to the Sino-German CRC 110 “Symmetries and the Emergence of Structure in QCD” (DFG Grant No. TRR110 and NSFC Grant No. 11621131001). This research used resources of ANL’s ATLAS facility, which is a DOE Office of Science User Facility.

### References

- [1] S. Frauendorf, Phys. Scr. 93 (4) (2018) 043003, <https://doi.org/10.1088/1402-4896/aaa2e9>.
- [2] S. Frauendorf, J. Meng, Nucl. Phys. A 617 (2) (1997) 131–147, [https://doi.org/10.1016/S0375-9474\(97\)00004-3](https://doi.org/10.1016/S0375-9474(97)00004-3).
- [3] A. Bohr, B.R. Mottelson, Nuclear Structure, vol. II, W. A. Benjamin, New York, 1975.
- [4] B.W. Xiong, Y.Y. Wang, At. Data Nucl. Data Tables 125 (2019) 193–225, <https://doi.org/10.1016/j.adt.2018.05.002>.
- [5] S. Ødegård, et al., Phys. Rev. Lett. 86 (26) (2001) 5866–5869, <https://doi.org/10.1103/PhysRevLett.86.5866>.
- [6] G. Schönwaßer, et al., Phys. Lett. B 552 (2003) 9–16, [https://doi.org/10.1016/S0370-2693\(02\)03095-2](https://doi.org/10.1016/S0370-2693(02)03095-2).
- [7] H. Amro, et al., Phys. Lett. B 553 (2003) 197–203, [https://doi.org/10.1016/S0370-2693\(02\)03199-4](https://doi.org/10.1016/S0370-2693(02)03199-4).
- [8] P. Bringel, et al., Eur. Phys. J. A 24 (2005) 167–172, <https://doi.org/10.1140/epja/i2005-10005-7>.
- [9] D.J. Hartley, et al., Phys. Rev. C 80 (2009) 041304, <https://doi.org/10.1103/PhysRevC.80.041304>.
- [10] J.T. Matta, et al., Phys. Rev. Lett. 114 (2015) 082501, <https://doi.org/10.1103/PhysRevLett.114.082501>.
- [11] S. Biswas, et al., arXiv:1608.07840v1 [nucl-ex], 2016.
- [12] J. Timár, et al., Phys. Rev. Lett. 122 (2019) 062501, <https://doi.org/10.1103/PhysRevLett.122.062501>.
- [13] I. Hamamoto, Phys. Rev. C 65 (2002) 044305, <https://doi.org/10.1103/PhysRevC.65.044305>.
- [14] S. Frauendorf, F. Dönau, Phys. Rev. C 89 (2014) 014322, <https://doi.org/10.1103/PhysRevC.89.014322>.
- [15] D.R. Jensen, et al., Phys. Rev. Lett. 89 (2002) 142503, <https://doi.org/10.1103/PhysRevLett.89.142503>.
- [16] D.C. Radford, Nucl. Instrum. Methods Phys. Res., Sect. A 361 (12) (1995) 297–305, [https://doi.org/10.1016/0168-9002\(95\)00183-2](https://doi.org/10.1016/0168-9002(95)00183-2).
- [17] J.T. Matta, Exotic Nuclear Excitations: The Transverse Wobbling Mode in  $^{135}\text{Pr}$ , Springer International Publishing, 2017.
- [18] N. Cieplicka, et al., Phys. Rev. C 86 (2012) 054322, <https://doi.org/10.1103/PhysRevC.86.054322>.
- [19] T. Yamazaki, Nucl. Data. Sect. A 3 (1967) 1, [https://doi.org/10.1016/S0550-306X\(67\)80002-8](https://doi.org/10.1016/S0550-306X(67)80002-8).
- [20] N. Sensharma, et al., to be published.
- [21] C.J. Chiara, et al., Phys. Rev. C 75 (2007) 054305, <https://doi.org/10.1103/PhysRevC.75.054305>.
- [22] J.A. Sheikh, K. Hara, Phys. Rev. Lett. 82 (1999) 3968–3971, <https://doi.org/10.1103/PhysRevLett.82.3968>.
- [23] J.A. Sheikh, et al., to be published.